



Research article

Annealing temperature variation and its influence on the self-cleaning properties of TiO₂ thin filmsV.T. Lukong^a, K. Ukoba^a, K.O. Yoro^{b,*}, T.C. Jen^a^a Department of Mechanical Engineering Science, University of Johannesburg, Auckland Park Campus, Auckland Park, 2092, Johannesburg, South Africa^b Energy Technologies Area, Lawrence Berkeley National Laboratory, 1 Cyclotron Road, Berkeley, CA, 94720, United States

ARTICLE INFO

Keywords:
 Annealing
 Self-cleaning
 Spin coating
 Thin film
 Titanium dioxide

ABSTRACT

Titanium dioxide (TiO₂) is an important material in science and engineering because of its basic and synthetic properties. Nevertheless, there is a dearth of reports in the open literature focusing on its ability to self-clean under temperature changes. In this study, we used the spin coating technique to produce TiO₂ thin films to evaluate its self-cleaning ability after annealing at different temperatures. The TiO₂ sol was obtained through an endothermal sol-gel process, and the gel was coated on a glass substrate using a spin coater. The deposited films were then annealed at 400 °C, 600 °C, and 800 °C for 1 h. The influence of annealing temperature variation on the self-cleaning properties of the thin film was characterized using X-ray diffraction, scanning electron microscope; Fourier transformed infrared spectrometric analysis and UV-vis spectrophotometer. A test to ascertain self-cleaning was conducted using the degradation of methylene blue, and the different films were tested for durability. The durability test confirmed the connection between solid coating and substrate at all annealing temperatures. Thin films annealed at 600 °C revealed the best self-cleaning properties. The morphological analysis revealed snowflake shapes uniformly distributed over the substrate at 400 °C, and agglomeration improved as the annealing temperature increased. Structural analysis showed an increase in crystallinity with an increase in annealing temperature for both rutile and anatase phases. At three different temperatures, the chemical bond and the absorption band pattern followed the same path, although the peak intensity declined with temperature rise. Finally, the optical bandgap of the thin coated TiO₂ declined from 3.39 eV to 3.20 eV as the binding temperature increased from 400 to 800 °C.

1. Introduction

The unique properties of Titanium dioxide (TiO₂) make it a point of attraction for many applications. It is the most readily available material for self-cleaning applications in window glass, self-cleaning membranes, and photovoltaic panels [1, 2, 3]. The use of TiO₂ is attractive because it is cheap, non-poisonous, odourless, non-flammable, and highly porous [4]. TiO₂ is soluble in water with a boiling point of 2972 °C and a high melting point of 1843 °C [5]. In addition, TiO₂ is chemically stable in the absence of light [6] and has a suitable bandgap for light absorption (3.0eV–3.2eV), making it a suitable charge carrier for both holes and electrons [7]. All these properties make TiO₂ highly favourable for self-cleaning applications, mainly because it becomes highly efficient in photocatalyzing dirt in the presence of sunlight.

TiO₂ exists in three phases; brookite, anatase, and rutile, of which anatase and rutile are the typical active phases. The rutile phase is the

most stable phase, with the highest refractive index of 2.609, and the anatase is the phase with the best photocatalytic behavior [8]. The brookite and anatase phases can easily be transformed into rutile structures by high-temperature annealing. Different ways of depositing TiO₂ thin films that are commonly employed include electron-beam evaporation [9], sol-gel spin coating method [10], Atomic layer deposition [11], magnetron sputtering [12], and spray pyrolysis [13]. Of these deposition procedures, the sol-gel spin-coated process is the most widely used. This could be attributed to the low cost of the sol-gel synthesis, which involves some chemical reactions to become a semisolid film. The significant supremacy of TiO₂ in self-cleaning procedures is its admirable features, consistency over substantial areas, and multidimensional processing capability.

Interests in the study of TiO₂ thin films and their applications have continued to rise in recent times. Several studies have been carried out to examine the influence of temperature on the internal properties of TiO₂.

* Corresponding author.

E-mail address: kelvin.yoroo@gmail.com (K.O. Yoro).

For example, the effects of temperature on the structure and optical properties of thin TiO₂ films have been studied in the past by Wong et al. (2017) [14]. The authors observed that the annealing temperature affects the structural and optical properties of the thin-film TiO₂. The researchers also reported that the crystal size and roughness of the surface of TiO₂ increase with incremental temperature change. The effects of temperature on the structure, morphology, and optical properties of thin TiO₂ films have been studied by Lin et al. (2013) [15]. The researchers concluded that an increase in annealing temperature changed TiO₂ thin films from amorphous to nanocrystalline anatase and that the bandgap dropped when the annealing temperature was elevated. Tański et al. (2018) [16] studied the influence of calcination temperature on TiO₂ thin films' optical and structural properties and observed a decrease in bandgap with an increase in calcination temperature. This drop in the bandgap between the valence and conduction band is an exciting factor in the self-cleaning property of TiO₂ that warrants further studies. Due to the photocatalytic activity generated by the absorption of sunlight, thin TiO₂ films placed on surfaces such as PV panels can be dispersed into dust and pollutants.

Upon being exposed to light, electrons in TiO₂ valence band become immobilized, moving to the conductance level, thereby leaving a negative valency (-e) behind. This immobilization leads to an electron-hole in the positive state (h⁺) that splits water molecules and produces hydrogen and its hydroxyls. By interacting with oxygen atoms, the electrons in the negative state (-e) generate binary oxide cations, and the phenomenon will continue if light exists. This is an indispensable aspect of TiO₂ that can be intensely utilized for self-cleaning and photocatalytic operations by immobilizing the TiO₂ on different suitable substrate surfaces. The microstructures of TiO₂ films are very critical to their final performance [17]. The alignment of these microstructures need to be controlled to obtain a TiO₂ thin film with quality properties. In their work, Al-Shomara and Alahmad (2019) [18] found that increasing annealing temperature from 0 to 600 °C resulted in a shift in the crystal plane (101) to higher values of 2 Theta degrees. The XRD peak intensities also increased as well as the crystallite size of the particles.

The main objective of this study is to determine the effects of temperature variations on the self-cleaning properties of TiO₂ thin films, and their self-cleaning behaviour. As far as we can determine, this has not been sufficiently reported in the literature. In addition, most studies in this field focused mainly on the effects of annealing temperature on the structural, optical, and morphological properties of TiO₂ thin films. In reality, when these parameters are changed, the self-cleaning function of the thin film is also influenced. Therefore, understanding how these modifications affect the TiO₂ thin films' self-cleaning ability is a huge contribution to the existing body of knowledge in photocatalytic applications of TiO₂. A novel heat-assisted sol-gel technique was used to prepare the transparent viscous films and then spin-coated on glass substrates. The morphological, structural, optical, and molecular bonding were investigated, followed by a self-cleaning and durability test. The bandgap of the different deposited films was determined, and conclusions were drawn based on the results obtained.

2. Experimental details

2.1. Materials

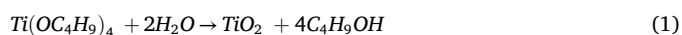
All compounds were procured as analytical grades and employed with no additional modification. The thin-film coating was carried out using glass plates purchased from Sigma Aldrich, South Africa. TiO₂ precursors and solvents are 97% Titanium isopropoxide (TTIP) and 99.9% ethanol, all purchased from Sigma Aldrich. The hydrolysis agent is ionized water, and the stabilizer is nitric acid supplied by Merck Chemicals also in South Africa.

2.2. Substrate preparation

Before being cleaned, the glass slides had to be trimmed to size (25 mm × 20 mm × 1 mm), washed with detergent, then ethanol, acetone and ionized water are added, and then dried for 15 min for 30 min in a 100 °C oven. Adequate cleaning of the substrates improves material-to-substrate adhesion and prevents contaminants from the formed coating.

2.3. TiO₂ sol preparation

The TiO₂ Sol was made by liquefying 97% TTIP in 99.90 % ethanol in a 1:5 volume proportion while stirring [19]. After 30 min of agitation, the acid stock, made of nitric acid and water at a ratio of 1:50 ratio, was poured drop-by-drop into the precursor mixture while stirring non-stop at 500 rpm with a magnetic stirrer to create a translucent gel. To ensure proper hydrolysis, the mixture was agitated for an additional 2 h at 60 °C under air pressure. Eq. (1) depicts the chemical synthesis of the TiO₂ gel.



2.4. The TiO₂ thin films deposition

A spin coater (Chemat KW-4A technology) was employed to coat the TiO₂ thin films. The statically applied solution onto the glass substrate was first spanned at 1000 rpm for 6 s, followed by a 3000-rpm speed for 30 s.

The lower speed assisted in spreading the solution evenly across the substrate's surface, whereas the greater pace helps the solution become thinner. The deposited films were then annealed at different temperatures of 400, 600, and 800 °C. The annealing at 800 °C was done in a patchy heat and cold manner for short periods until one hour to avoid the glass substrate from melting.

2.5. Characterization of the coated film

A TESCAN VEGA3 OXFORD scanning electron microscope was used to analyze morphologies. The elemental composition was validated using an Aztec instrument (OXFORD) EDX Spectrometer, while the structural characteristic was investigated using an XPERT-PRO (Philips) X-ray for 2θ angles ranging from 5 to 90° with CuKα X-ray of wavelength λ = 1.54056 Å. The optical characteristics of the deposited films were investigated with a scan rate of 600 nm/min on a UV-2450 (SHIMADZU) Spectrochrometer in wavelengths ranging from 200 to 600nm. A Perkin Elmer Spectrum 100 FT-IR spectrophotometer was used to examine the thin films' chemical bonding and absorption bands in the spectrum range of 300–4000 cm⁻¹. Testing for the self-cleaning capability of the deposited films was conducted with methylene blue staining and then exposed to visible light irradiation for two hours. The adhesion cross-hatch test was used to determine the durability of the product. The entire experimental steps and critical steps followed in this study are shown in Figure 1.

3. Results and discussion

3.1. Elemental composition

Figure 2 shows the elemental composition of the TiO₂ deposited thin films and annealed at 400 °C. The image obtained from EDX examination reveals Titanium (Ti) and Oxygen (O₂) present in a larger bulk fraction. Some constituents of the glass substrates such as Sodium (Na), Calcium (Ca), Carbon(C), and Silicon (Si) appear in the EDX analysis but with a lower weight percentage. Lukong et al. (2022) [20] achieved a similar

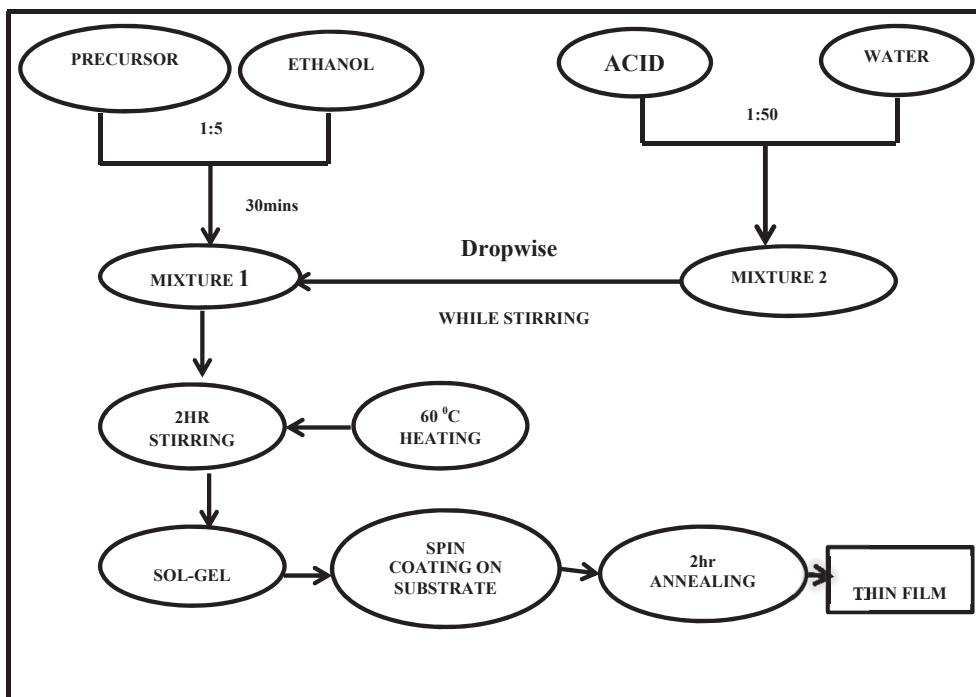


Figure 1. Experimental process and critical steps of the study. Adapted and modified from Lukong et al [20], with permission from Elsevier Under the license Creative Commons CC-BY-NC-ND.

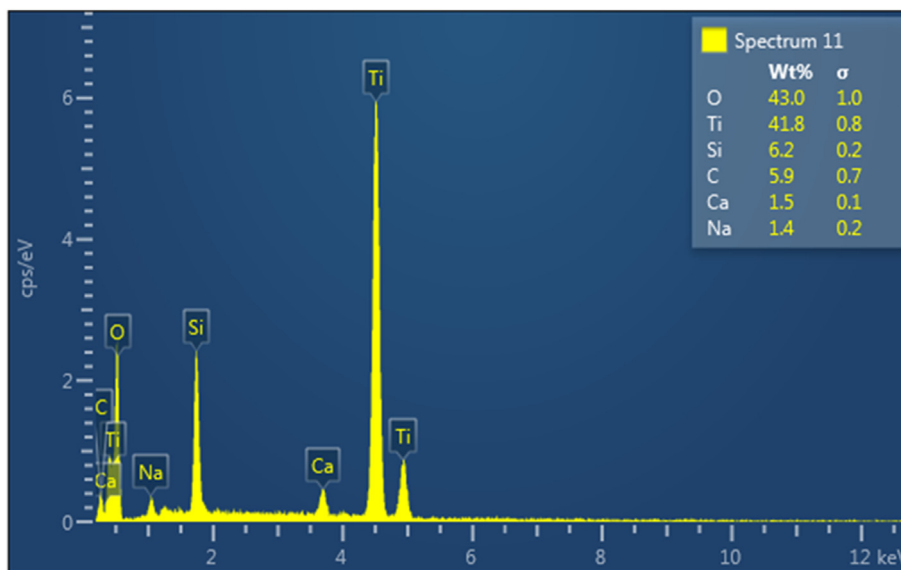


Figure 2. EDX image of coated TiO₂ film after annealing at 400 °C. Adapted from Lukong et al [20], with permission from Elsevier Under the license Creative Commons CC-BY-NC-ND.

result. The EDX analysis revealed a molecular weight percentage of 41.8 % for Ti and 43.0 % for O, which compares well to theoretical values of 40.07 % for O and 59.93 % for Ti in the TiO₂ mix, in the absence of any impurity, confirming the strong presence of TiO₂ in proper measures in the thin films [21]. Thermal subjection often activates the diffusion of silicon and Sodium from the TiO₂ thin film in the glass substrate [22].

3.2. Morphological studies

The morphologies of the TiO₂ thin films annealed at 400, 600, and 800 °C were studied using scanning electron microscope (SEM). The SEM micrograph obtained for the three different coatings is displayed in

Figure 3. At the annealing temperature of 400 °C, the particles had snowflake structures evenly distributed over the substrate. Snowflake structures are almost six-sided and have gaps within their ranks. These gaps help to expose more surface of the particle to sunlight, thus enlarging the area of sunlight energy absorption on the surface of the particle. The thin film annealed at 600 °C shows the particle agglomerated at certain points over the substrate surface. Smaller particles in the nanometer range are seen scattered in between the agglomerated ones. At 800 °C of annealing temperature, the particle splatters on the glass substrate, increasing the size of the agglomeration. The highest porosity shows that the pore volume increases, and the surface area diminish as the annealing temperature increases. The soft and robust agglomerates

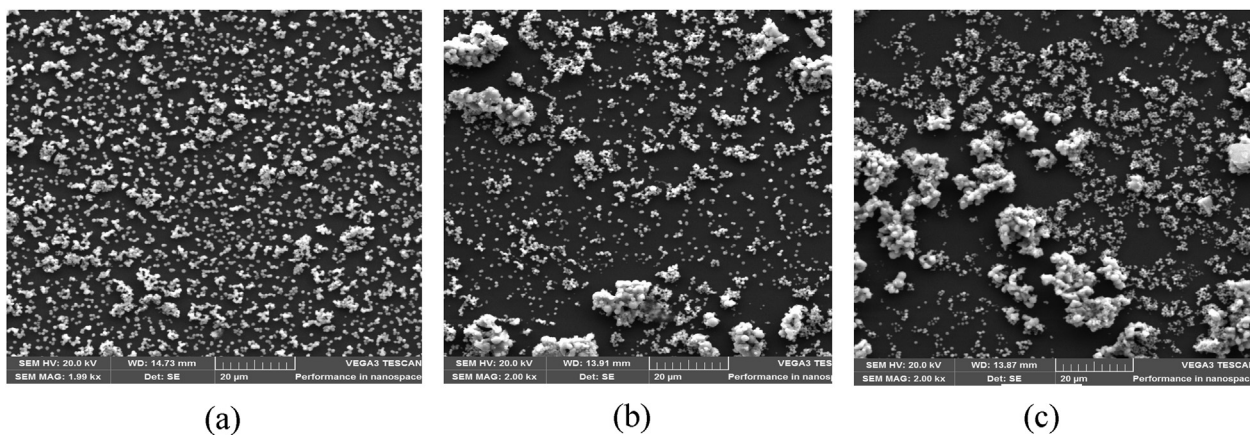


Figure 3. SEM images of deposited TiO₂ thin films annealed at (a) 400 °C, (b) 600 °C, and (c) 800 °C. (a) was adapted from Lukong et al [20], with permission from Elsevier Under the license Creative Commons CC-BY-NC-ND.

result from the weak capillary forces and strong molecular bonds pulling the small particles together to create larger ones on the substrate surface. Several authors had reported similar morphological displays when they varied annealing temperatures, some with different particle shapes [23, 24]. The snowflake shapes of the particle are more significant at 800 °C, bringing out a well-open surface that encourages the adsorption of an esteemed spectrum of solar energy per unit area of the surface, which is a desirable property for self-cleaning and photocatalytic activities.

3.3. Structural and phase analysis

Figure 4 shows the X-ray diffraction patterns of the deposited TiO₂ thin film, which were bound at different temperatures of 400, 600, and 800 °C for 2 Theta degrees from 10 to 80. The result reveals tetragonal anatase crystal structures with broad peaks for the film annealed at 400 °C (matching ICDD card no. 01-070-6826). No rutile phases were present at 400 °C. The tetragonal anatase phase had peaked at 2 Theta degrees of 25.42, 38.14, 47.98, 54.34, 55.29, and 63.09, relating to (h k l) crystal levels of (101), (004), (200), (211), and (204) in that order. For TiO₂ thin films annealed at 600 °C, the tetragonal anatase phase shows improved crystallinity with sharper and higher peak intensities. Few rutile phases with low intensity are also present at 2 Theta degrees of 27.38, 36.08, 41.22, and 56.51 relating to (h k l) crystal planes of (110), (101), (111), and (220) respectively according to ICDD card no 04-003-0648. The

appearance of the rutile phase at 600 °C can be attributed to the longer annealing time of one hour that could create enough heat energy to effect phase transformation [25]. The XRD pattern for TiO₂ coated film heat-treated at 800 °C shows the presence of both anatase and rutile phases with higher peak intensities. The molar proportion of anatase (101) to rutile (110) phase was evaluated from the most intense XRD peaks of both phases by Myers and Spurr method [26] using Equations [2] and [3].

$$M_R = \frac{1}{[1 + 0.8(PA/PR)]} \quad (2)$$

$$M_A = 1 - M_R \quad (3)$$

where M_R and M_A signify the molar proportions of the rutile and anatase phases, respectively, P_R and P_A denote the rutile and anatase peak intensities. The results recorded in Table 1 show that as the annealing temperature is raised, the anatase concentration decreases, and the rutile content increases. It also depicts the complementary relationship between the two phases.

This finding also supports the idea that heat treatment can control rutile and anatase molar fraction, as well as phase transformation.

The average crystallite dimension for the various coated films was evaluated using the Debye-Scherrer formula [27] shown in Equation [4].

$$D = \frac{k\lambda}{\beta \cos \theta} \quad (4)$$

With λ representing the X-ray wavelength of Cu-k radiation (nm), β is the full width of a maximum of half (FWHM) obtained in the radians, θ represents the Bragg diffraction angle and k is a forming constant (0.9). At an annealing temperature of 400 °C, the anatase TiO₂ film crystallite size varied from 4.19 to 5.13 nm. The crystallite size for anatase TiO₂ coated film annealed at 600 °C had the lowest possible value of 18.29 nm and a maximum of 20.23 nm. The anatase phase at 800 °C had crystallite sizes ranging from 22.78 to 24.69 nm, an average crystallite value of 23.95 nm, and the rutile phase crystals had sizes from 31.37 to 36.85 nm.

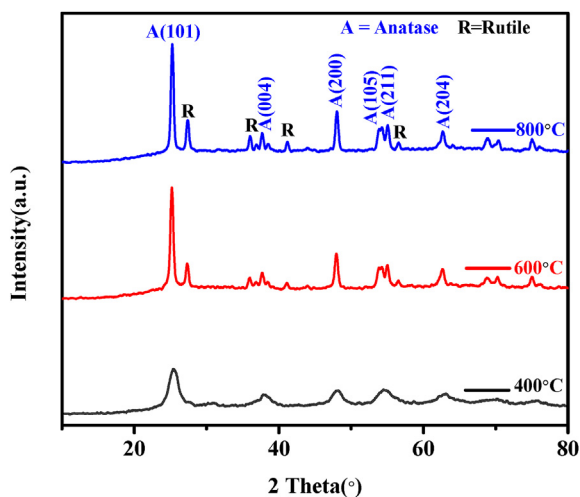


Figure 4. X-ray diffraction patterns of thin TiO₂ films at 400, 600, and 800 °C are coated.

Table 1. Variation of mole fraction of anatase and rutile with annealing temperature.

Annealing Temperature	400 °C	600 °C	800 °C
Molar Proportions			
M_A	1	0.7032	0.6738
M_R	0	0.2968	0.3262

The evaluated average crystallite sizes for the rutile and anatase phases of the TiO₂ thin films alongside its properties for the three different annealing temperatures investigated in this study are outlined in Table 2.

From the information available in Table 2, it is observed that as the annealing temperatures were raised from 400 °C to 800 °C, the crystallite size for anatase and rutile phases also increased. The largest crystallite size of 34.59 nm was evaluated for rutile tetragonal structure at 800 °C. This finding is consistent with Haq et al.'s (2018) [28] result for varying annealing temperatures up to 900 °C. Although the crystallinity remained tetragonal for the different annealing temperatures and all the phases, the sharp peaks at 600 °C and 800 °C show the particles are better crystalline than at 400 °C. A better crystalline structure and particles with snowflake shapes improve self-cleaning properties and photocatalytic function of TiO₂ thin films because suitable crystal anatomies mean fewer crystal flaws and a peak surface to volume ratio, that minimizes the rate of recombination of electron hole [29].

3.4. Molecular bonding and absorption bands analysis

The molecular bonding and absorption bands of the TiO₂ thin films obtained for various annealing temperatures were analyzed using FTIR spectroscopy, and the results are shown in Figure 5. All patterns for the three different temperatures followed the same trajectory, but the peak intensities decreased as the temperature increased. Prominent peaks are seen in the range of 2950.37 cm⁻¹ to 2840.10 cm⁻¹ and the field of 1732.49 cm⁻¹ to 840.51 cm⁻¹. The heat treatment helped in burning out most of the hydroxyl groups. This is shown by the weak decreasing peak intensity of O–H stretching vibration at 3750.86 cm⁻¹ due to the disappearing hydroxyl groups [30]. The C–H stretching vibration is seen from 2950.31 cm⁻¹ to 2840.10 cm⁻¹. The sharp peaks at 1448.95 cm⁻¹ and 1372.21 cm⁻¹ are attributed to O–H in-plane bending vibrations. The absorption at 1166.43 cm⁻¹ is relatable to the C–O stretching vibration. The broad bending bands around 957.71 cm⁻¹, 840.10 cm⁻¹, and 799.69 cm⁻¹ can be attributed to Ti–O, Ti–O–Ti, and O–Ti–O, respectively [31]. The significant absorption peaks indicate the carboxylic group's strong presence and stability in stretching and the hydroxyl in bending vibrations. Different functional groups in TiO₂ thin films at all annealing temperatures will influence their molecular absorption performance [32]. As the annealing temperature increases, there is a shift of the pattern towards the stretching vibration bands and a decrease in peak intensity that could be due to the elimination of impurities and better crystallization of the TiO₂ structure. Chacko and Aneesh (2018) [33] have reported similar findings.

3.5. Optical properties analysis

The optical analysis of thin film coated with titanium dioxide heat-treated at 400 °C, 600 °C, and 800 °C is shown in Figure 6. Figures 6 (a) and 6(b) show the absorption spectra and linearity of the Tauc plot of $(\alpha h\nu)^2$ versus incident photon ($h\nu$) respectively. The optical bandgap for the direction allowed transition for the prepared TiO₂ thin films was plotted using data from UV-2450 (SHIMADZU) spectrophotometer and Tauc's relation [34] shown in Eq. (5).

$$(\alpha h\nu)^n = K(h\nu - E_g) \quad (5)$$

Table 2. The phase, crystal form and average crystallite size of TiO₂ thin films at different annealing temperature.

Annealed temperature (C)	Phase	Crystallinity	Average crystalline size (nm)
400	Anatase	Tetragonal	4.77
600	Anatase	Tetragonal	19.49
	Rutile	Tetragonal	30.61
800	Anatase	Tetragonal	23.95
	Rutile	Tetragonal	34.59

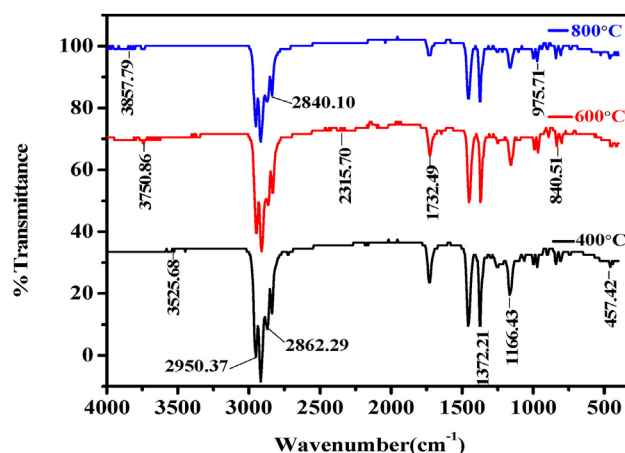


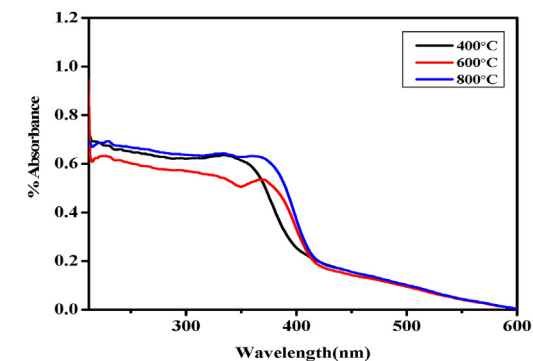
Figure 5. FTIR bands of TiO₂ coated film annealed at 400 °C, 600 °C, and 800 °C.

E_g indicates the optical bandgap of the created films, $h\nu$ denotes the incident energy of the photon, ' α ' stands for the absorption coefficient calculated with the help of Beer-Lambert's law, and K is a constant independent of energy. The value of the symbol n is determined by the type of transition (For a direct allowable change, $n = 2$). A plot of $(\alpha h\nu)^2$ versus $(h\nu)$ between 200 nm and 600 nm showed that the TiO₂ coated films absorbed highly in the visible light spectrum for all the thin films annealed at different temperatures. As shown in Figure 5(a), the produced thin film absorbed UV radiation with wavelengths of 420 nm and below. It is observed that as the annealing temperature increased, the absorption shifted to higher wavelengths. This is necessary to accommodate the required absorption. At higher temperatures, increasing crystal size, as XRD results show, means that small surfaces are exposed to light absorption. With smaller crystallite sizes, such as at 400 °C, a large specific surface area is exposed to light absorption. This is the capability of anatase TiO₂ allows more photons to be energized and boosts the power conversion efficiency of the solar panel [35].

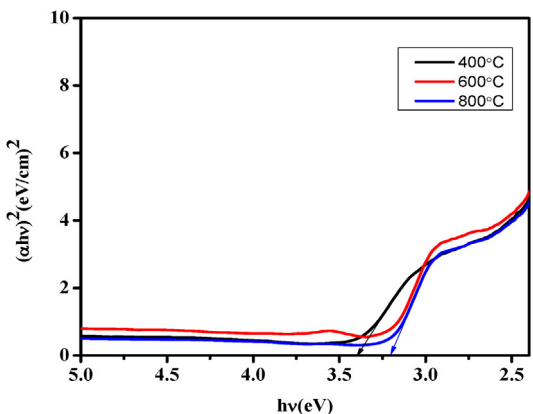
As shown in Figure 5, the bandgap was calculated by stretching the tangent from the right part of the curve to the horizontal axis. The direct bandgap analysis of the coated film showed that after increasing the temperature of annealing from 400 C to 800 C, the rate dropped from 3.39 eV to 3.20 eV. This value is consistent with the phase change of anatase to rutile as the temperature of the annealing was increased. The lower band distance is suitable for self-cleaning applications, as this film is functional quickly once it is exposed to visible light. This is because less energy is needed to move from valence to the conducting band, resulting in higher photocatalytic activity. In the work of Sarode et al. (2012) [36] and Ranjitha et al. (2013) [37], similar results were observed in the TiO₂ bandgap when the annealing temperature varied between 100 and 500 °C. Annealing aids in the removal of internal stresses in coatings that may have been formed during the deposition stage, thereby improving the film's crystal anatomy. The bandgap of the coated film will be optimized because of this enhancement in the crystal structure. The Envelope method was used to establish the thickness and refractive index of the coated film [38]. The refractive index and thickness of thin films formed on glass substrates are calculated with equations [6] and [7]. The variable N in the refractive index formula depends on the type of absorption and is determined using Equation [8] for medium and weak absorption.

$$n = \left[N + (N^2 - S^2)^{1/2} \right]^{1/2} \quad (6)$$

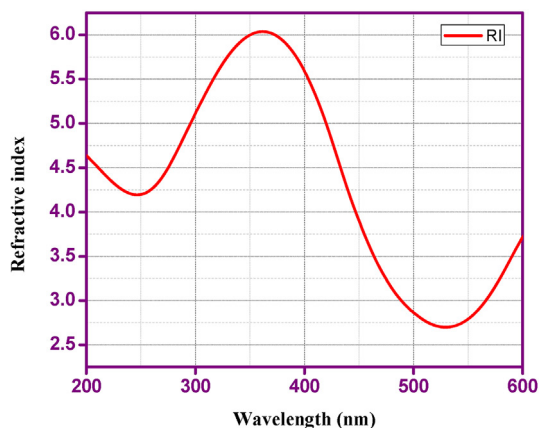
$$d = \frac{\lambda_1 \lambda_2}{2(\lambda_1 n_2 - \lambda_2 n_1)} \quad (7)$$



(a)



(b)



(c)

Figure 6. Analysis of the optical properties of the coated TiO₂ thin films; (a) Absorbance spectra of the films at the different annealing temperatures, (b) bandgap analysis of the thin films annealed at 400°C, 600°C, and 800°C, (c) Refractive index plot against the wavelength of TiO₂ thin film annealed at 600 °C.

However, for medium and weak absorption,

$$N = 2S \left(\frac{TM - Tm}{TMTm} \right) + (S^2 + 1) / 2 \tag{8}$$

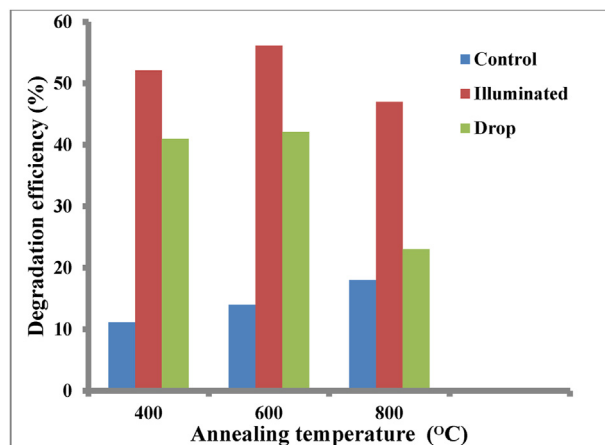


Figure 7. Methylene blue degradation efficiency of TiO₂ thin films annealed at varying temperatures.

Where *n* denotes the TiO₂ thin film's refractive index, *d* is film width, *T_m* represents the minima, and *T_M* represents the maxima of transmittances in the envelope plot at a given wavelength, *S* is the refractive index of the substrate, which is 1.51 for glass, 1 and 2 are respectively wavelengths and refractive indices for two nearby maxima or minima. Figure 6 (c) shows the refractive index of the sample which has been annealed at 600 °C plotted against its wavelength. The coated TiO₂ thin film was established to have a thickness of 63 nm. The refractive index curve's higher values implies good optical application features, as this indicates significant absorption capability [39].

3.6. Self-cleaning test

For the self-cleaning test, the efficiency of each prepared thin film to degrade methylene blue under visible light was investigated. Methylene blue solution (100ppm) was applied as a contaminant onto the surfaces of the coated thin films. Following that, the films were exposed to visible light (72 W) for four hours in a closed chamber, while control samples stained with methylene blue were kept in the dark for the same length of time. The absorbance values of the specimens were recorded before being stained with methylene blue and after visible light exposure; the absorbance measurements were recorded again to assess the self-cleaning ability. The setup was so that the percentage of methylene blue degradation of the thin films annealed at the different temperatures will be compared with the control sample to determine which annealing temperature had the optimal photocatalytic activity or the highest methylene blue degradation efficiency. The maximum absorbance peak record was taken for each thin film at the different annealed temperatures, and its percentage degradation was calculated with reference to the control sample to generate a methylene blue degradation curve according to Equation [9].

$$\%D = \frac{C_0 - C_t}{C_0} \times 100\% \tag{9}$$

Where %D is the degradation efficiency, *C₀* is the methylene blue concentration at the beginning, and *C_t* represents methylene blue concentration after visible light exposure on the thin film at the annealed temperature. The results shown in Figure 7 revealed that photocatalytic activity improved as the annealing temperature was raised, with the maximum efficiency obtained at an annealing temperature of 600 °C, after which there was a drop-in photocatalytic activity as seen with the thin film annealed at 800 °C. This could somewhat be attributed to the formation of better crystalline anatase structures at 600 °C because the specific surface area of the TiO₂ thin increased, leading to the creation of more reactive sites to absorb methylene blue [40]. When the annealing

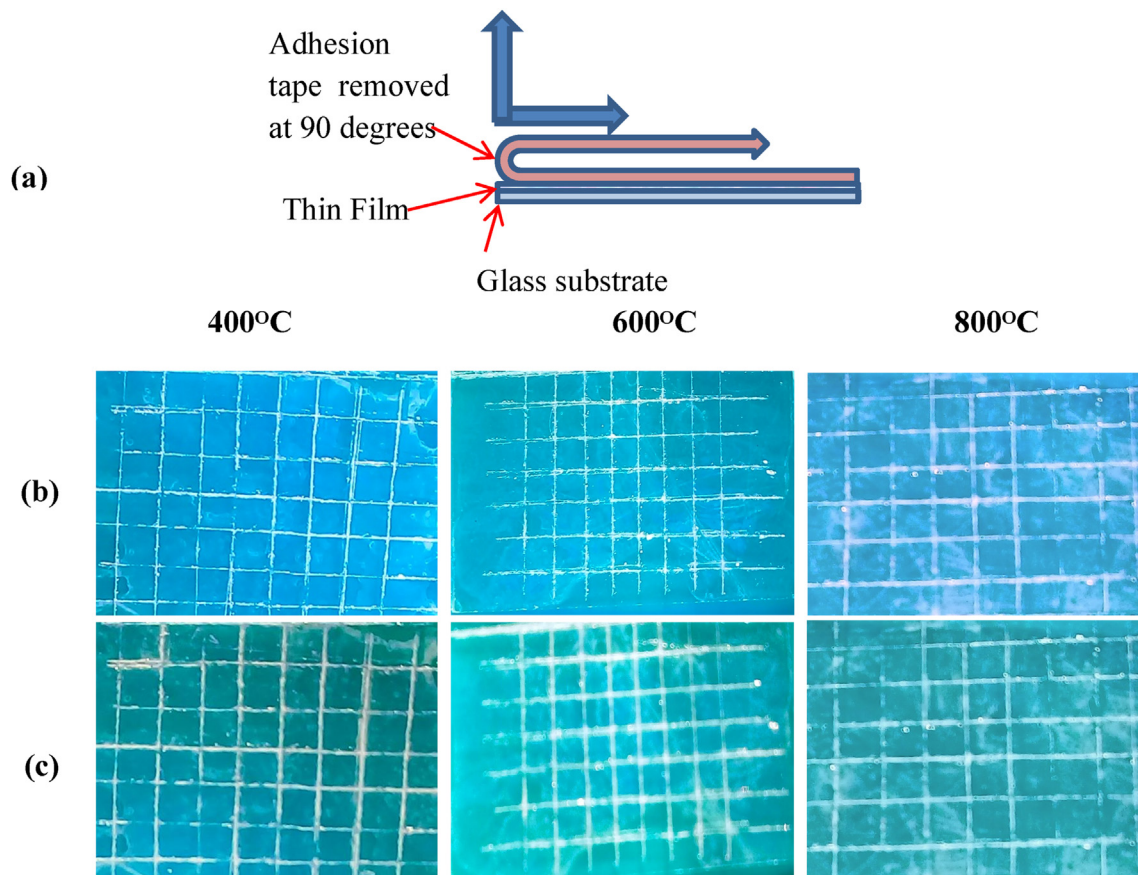


Figure 8. Thin-film durability test analysis; (a) Setup of how to remove the adhesion tape from the thin film surface, (b) Surface of crosshatched TiO_2 thin film before application of adhesion tape, (c) Appearance of the TiO_2 thin film after removal of adhesion tape. (a) and (b) were adapted from Lukong et al [20], with permission from Elsevier Under the license Creative Commons CC-BY-NC-ND.

temperature increased to 800 °C, the increase in rutile phase intensity and crystallite size limited the surface area in contact with the catalyst, thereby reducing the photocatalytic activity [41]. Optimal photocatalytic actions are desired in self-cleaning applications. Several authors, including Liang et al. (2018) [42], have reported similar results for sol-gel synthesized and spin-coated TiO_2 thin films under various annealing temperature variations.

3.7. Durability test

A durability test was performed to understand the strength of the bond between the substrate and the coating. Such a test indicates how the thin film will withstand distortions due to harsh environmental conditions such as dust and sand crashes, heavy rainfall with hailstones, impact from heavy winds and falling objects, corrosive materials, and other environmental hazards. The adhesion crosshatch method was used to perform the test, and the data obtained were analyzed according to ISO 9211-4 grade.

On each specimen, six equidistant lines 2 mm aside were cut using a nickel-gilded diamond glasscutter (Z169064-1EA) from Sigma-Aldrich. Then, to produce a crosshatched pattern, another set of six equidistant lines 2 mm from each other were slashed perpendicularly across the other set of six. The crosshatch pattern was scrutinized for irregularities before the adhesive tape from ISADEAL SA was gently applied evenly on top of it and firmly rubbed on the coated film surface with a finger on the non-sticky side. After that, the specimen was gripped solidly in one hand while the sticky tape was slowly and steadily withdrawn from the specimen surface at a 90-degree angle. Before the application of the tape, the specimen was inspected for damage, bare blotches, strange particles,

cracks, and other abnormalities that might influence the results. The sample was examined under transmitted light with unassisted eyes for coating removal after the tape had been removed, in accordance with ISO 14997.

Figure 8 depicts the results of the various thin-film durability tests. After cross-hatching the thin films, adhesion tape was applied firmly to the hatched surface and removed quickly in the manner depicted in Figure 8(a). Figures 8(b) and 8(c) are zoomed images of the appearance of the coated TiO_2 films before and after the application of the sticky tape, respectively. In line with ISO 9211-4, the film is rated from 0 to 5 depending on the detachment of the coating after the application and removal of the adhesion tape. The value zero implies that the cuts' edges are completely smooth and none of the squares of the lattice is detached. This indicates a strong bond between the coating and the substrate. A mark of 5 indicates severe coating separation and flaking, as well as a weak coating-to-substrate bond. By comparing Figure 8(c) to 8(b), it is observed that after placing and withdrawing the sticky tape on all thin films, a very small crack occurred on the TiO_2 coatings. The edges of the cuts and lattice squares showed a decrease of less than 5% for the thick film coated with 400 and 600 °C. Although there were few drops at the intersections of the hatched lines, there were some flakes at the intersections of the hatched lines. The hatchings' faults at the borders of the cuts and cross points can be traced to the diamond cutter's handling during the hatchings' creation. The absence of a coating section of less than 5% demonstrates that the coating of TiO_2 thin films is difficult to remove and therefore durable, as mandated by the ISO 9211-4 requirements. These findings tally with Womack et al. (2019) [43] to test anti-reflective coatings' durability on solar cell coverings. However, the thin film was annealed at 800 °C although had a solid coating to the

substrate bond; the high annealing temperature made the glass substrate more brittle, implying that such thin films will not withstand substantial impacts. Greater than 5% flaking of the coated films was also observed within the lattice squares for thin film annealed at 800 °C, revealing that the adhesion tape removed more material. This could be because as the glass substrate became brittle, it melted within its ranks during the annealing and led to invisible defects such as cracks within the coating, making it quickly removed by the adhesion tape. A slight colour change due to residual leftover was observed on all thin films after applying the adhesion tape, as seen in Figure 8(c). Afzal et al. (2021) [44] noted that in addition to its self-cleaning capabilities, TiO₂ coatings harden solar cell covers preventing them from scratches and other physical damage. In the self-cleaning technology industry, constructing self-cleaning surfaces using low-cost and simple approaches has proven to be a challenge [45]. As a result, this outcome provides a first step towards conquering this obstacle.

4. Conclusions

In this study, thin-film TiO₂ has been successfully deposited onto a glass substrate via a liquid-gel and rotation coating process. The influence of the temperature variation of the anode on the self-cleaning property of the TiO₂ film was studied for structural, morphological, optical, and photocatalytic activities. The morphological analysis revealed a snowflake shape that is uniformly distributed over the substrate at 400 °C and agglomerated as the annealing temperature increased. EDX analysis showed that Titanium and Oxygen atoms were strongly present in the thin films with higher percentage weights, while the FTIR analysis confirmed a substantial presence of TiO₂. Crystallite sizes of 4.77nm, 19.49 nm, and 23.95 nm were obtained in the anatase phase at 400, 600, and 800 °C, respectively, showing that the size increases with incremental annealing temperature.

In addition, the optical band decreased from 3.39 eV to 3.20 eV when the annealing temperature was raised from 400 °C to 800 °C. Self-cleaning tests confirmed that TiO₂ thin films annealed at 600 °C have the highest efficiency of methylene blue decomposition, while the durability test revealed that the TiO₂ thin film annealed at all the temperatures had a solid substrate to coating bond. However, the 800 °C annealing temperature made the glass substrate more brittle.

Finally, it can be inferred that raising the annealing temperature increases the photocatalytic properties, and thus the self-cleaning capability of the thin film. Findings from this study will be immensely helpful in designing future self-cleaning coatings for photovoltaic applications with TiO₂ as a major material.

Declarations

Author contribution statement

V.T. Lukong: Performed the experiments; Wrote the paper.
 K. Ukoba: Conceived and designed the experiments.
 K.O. Yoro: Analyzed and interpreted the data.
 T.C. Jen: Contributed reagents, materials, analysis tools or data.

Funding statement

This research did not receive any specific grant from funding agencies in the public, commercial, or not-for-profit sectors.

Data availability statement

Data will be made available on request.

Declaration of interests statement

The authors declare no conflict of interest.

Additional information

No additional information is available for this paper.

References

- [1] H.E. Doghmane, T. Touam, A. Chelouche, F. Challali, D. Djouadi, Synthesis and Characterization of TiO₂ Thin Films for Photovoltaic and Optoelectronic Applications in ICREEC 2019, Springer, Singapore, 2020, pp. 311–317.
- [2] Y. Liang, S. Sun, T. Deng, H. Ding, W. Chen, Y. Chen, The preparation of TiO₂ film by the sol-gel method and evaluation of its self-cleaning property, *Materials* 11 (3) (2018) 450.
- [3] S. Rempe, J.C. Brinker, D.M. Rogers, Y.B. Jiang, S. Yang, Biomimetic Membranes and Methods of Making Biomimetic Membranes (No 10,130,916, Sandia National Laboratories (SNL), Albuquerque, NM, and Livermore, CA (United States), 2018.
- [4] K. Maeda, A. Xiong, T. Yoshinaga, T. Ikeda, N. Sakamoto, T. Hisatomi, M. Takashima, D. Lu, M. Kanehara, T. Setoyama, T. Teranishi, Photocatalytic overall water splitting promoted by two different cocatalysts for hydrogen and oxygen evolution under visible light, *Angew. Chem.* 122 (24) (2010) 4190–4193.
- [5] M. Khan, Z. Yi, U. Fawad, W. Muhammad, A. Niaz, M.I. Zaman, A. Ullah, Enhancing the photoactivity of TiO₂ by co-doping with silver and molybdenum: the effect of dopant concentration on the photoelectrochemical properties, *Mater. Res. Express* 4 (4) (2017) 45023.
- [6] Y. Liang, H. Ding, Q. Xue, Characterization of Brucite/TiO₂ composite particle material prepared by Mechano-chemical method, *Surf. Rev. Lett.* 25 (4) (2018) 1850085.
- [7] G. Nagaraj, A. Irudayaraj, R.L. Josephine, Tuning the optical band Gap of pure TiO₂ via photon induced method, *Optik* 179 (2019) 889–894.
- [8] S. Segota, L. Čurković, D. Ljubas, V. Svetličić, I.F. Houra, N. Tomašić, Synthesis, characterization and photocatalytic properties of sol-gel TiO₂ films, *Ceram. Int.* 37 (4) (2011) 1153–1160.
- [9] A. Taherniya, D. Raoufi, The annealing temperature dependence of anatase TiO₂ thin films prepared by the electron-beam evaporation method, *Semicond. Sci. Technol.* 31 (12) (2016) 125012.
- [10] T. Tański, W. Matysiak, D. Kosmalka, A. Lubos, Influence of Calcination Temperature on Optical and Structural Properties of TiO₂ Thin Films Prepared by Means of Sol-Gel and Spin Coating, *Bulletin of the Polish Academy of Sciences: Technical Sciences*, 2018, pp. 151–156.
- [11] P.O. Oviroh, R. Akbarzadeh, D. Pan, R.A.M. Coetzee, T.C. Jen, New development of atomic layer deposition: processes, methods and application, *Sci. Technol. Adv. Mater.* 20 (1) (2019) 465–496.
- [12] J.P. Vilcot, B. Ayachi, T. Aviles, P. Miska, Full sputtering deposition of thin film solar cells: a way of achieving high efficiency sustainable tandem cells? *J. Electron. Mater.* 46 (11) (2017) 6523–6527.
- [13] K.O. Yoro, M.O. Daramola, P.T. Sekoai, E.K. Armah, U.N. Wilson, Advances and emerging techniques for energy recovery during absorptive CO₂ capture: a review of process and non-process integration-based strategies, *Renew. Sustain. Energy Rev.* 147 (2021) 111241.
- [14] A. Wong, W.A. Daoud, H. Liang, Y.S. Szeto, The effect of aging and precursor concentration on room-temperature synthesis of nanocrystalline anatase TiO₂, *Mater. Lett.* 117 (2014) 82–85.
- [15] C.P. Lin, H. Chen, A. Nakaruk, P. Koshy, C.C. Sorrell, Effect of annealing temperature on the photocatalytic activity of TiO₂ thin film, *Energy Proc.* 34 (2013) 627–636.
- [16] T. Tański, W. Matysiak, D. Kosmalka, A. Lubos, Influence of Calcination Temperature on Optical and Structural Properties of TiO₂ Thin Films Prepared by Means of Sol-Gel and Spin Coating, *Bulletin of the Polish Academy of Sciences: Technical Sciences*, 2018, pp. 151–156.
- [17] M. Alzamani, A. Shokuhfar, E. Eghdam, S. Mastal, Study of annealing temperature variation on the structural properties of dip-coated TiO₂-SiO₂ nanostructured films, *Iran. J. Mater. Sci. Eng.* 10 (1) (2013) 39–45.
- [18] S.M. Al-Shomara, W.R. Alahmad, Annealing temperature effect on structural, optical and photocatalytic activity of nanocrystalline TiO₂ films prepared by sol-gel method used for solar cell application, *Digest J. Nanomater. Biotechnol.* 14 (2019) 617–625.
- [19] V.T. Lukong, K.O. Ukoba, T.C. Jen, Analysis of sol aging effects on self-cleaning properties of TiO₂ thin film, *Mater. Res. Express* 8 (10) (2021) 105502.
- [20] V.T. Lukong, R.T. Mouchou, G.C. Enebe, K. Ukoba, T.C. Jen, Deposition and characterization of self-cleaning TiO₂ thin films for photovoltaic application, *Mater. Today Proc.* (2022).
- [21] M.K. Hossain, M.F. Pervez, M.N.H. Mia, S. Tayyaba, M.J. Uddin, R. Ahamed, R.A. Khan, M. Hoq, M.A. Khan, F. Ahmed, Annealing temperature effect on structural, morphological and optical parameters of mesoporous TiO₂ film photoanode for dye-sensitized solar cell application, *Mater. Sci.* 35 (2017) 868–877.
- [22] J. Libardi, K.G. Grigorov, M. Massi, A.S. da Silva Sobrinho, R.S. Pessoa, B. Sismanoglu, Diffusion of silicon in titanium dioxide thin films with different degree of crystallinity: efficiency of TiO₂ and TiN barrier layers, *Vacuum* 128 (2016) 178–185.
- [23] F.N. Mohamed, M.S.A. Rahim, N. Nayan, M.K. Ahmad, M.Z. Sahdan, J. Lias, Influence of TiO₂ Thin Film Annealing Temperature on Electrical Properties Synthesized by CVD Technique, *Doctoral dissertation, Universiti Tun Hussein Onn Malaysia*, 2015.
- [24] K. Manickam, V. Muthusamy, S. Manickam, T.S. Senthil, G. Periyasamy, S. Shanmugam, Effect of annealing temperature on structural, morphological and

- optical properties of nanocrystalline TiO₂ thin films synthesized by sol-gel dip coating method, *Mater. Today Proc.* 23 (2020) 68–72.
- [25] A.S. Bakri, M.Z. Sahdan, F. Adriyanto, N.A. Raship, N.D.M. Said, S.A. Abdullah, M.S. Rahim, January. Effect of annealing temperature of titanium dioxide thin films on structural and electrical properties, in: *AIP Conference Proceedings 1788*, AIP Publishing LLC, 2017, p. 30030. No. 1.
- [26] R.A. Spurr, H. Myers, Quantitative analysis of anatase-rutile mixtures with an X-ray diffractometer, *Anal. Chem.* 29 (5) (1957) 760–762.
- [27] A. Valério, S.L. Morelha, Usage of Scherrer's Formula in X-ray Diffraction Analysis of Size Distribution in Systems of Monocrystalline Nanoparticles, 2019 arXiv preprint arXiv:1911.00701.
- [28] S. Haq, W. Rehman, M. Waseem, R. Javed, M. Shahid, Effect of heating on the structural and optical properties of TiO₂ nanoparticles: antibacterial activity, *Appl. Nanosci.* 8 (1) (2018) 11–18.
- [29] M.R.A. Abad, S.F. Shayesteh, H.F. Shayesteh, Effect of synthesis conditions on the structural, photocatalytic, and self-cleaning properties of TiO₂ nanoparticles, *Phys. Solid State* 62 (1) (2020) 120–130.
- [30] S. Sharma, A.V.D. Reddy, N. Jayarambabu, N.V.M. Kumar, A. Saineetha, K.V. Rao, S. Kailasa, Synthesis and characterization of Titanium dioxide nanopowder for various energy and environmental applications, *Mater. Today Proc.* 26 (2020) 158–161.
- [31] R. Singh, S. Dutta, Synthesis and characterization of solar photoactive TiO₂ nanoparticles with enhanced structural and optical properties, *Adv. Powder Technol.* 29 (2) (2018) 211–219.
- [32] J. Feng, Y. Liu, L. Zhang, J. Zhu, J. Chen, H. Xu, H. Yang, W. Yan, Effects of calcination temperature on organic functional groups of TiO₂ and the adsorption performance of the TiO₂ for methylene blue, *Separ. Sci. Technol.* 55 (4) (2020) 672–683.
- [33] L. Chacko, P.M. Aneesh, Effect of growth techniques on the structural and optical properties of TiO₂ nanostructures, *Mater. Res. Express* 5 (1) (2018) 15031.
- [34] D. Komaraiah, P. Madhukar, Y. Vijayakumar, M.R. Reddy, R. Sayanna, Photocatalytic degradation study of methylene blue by brookite TiO₂ thin film under visible light irradiation, *Mater. Today Proc.* 3 (10) (2016) 3770–3778.
- [35] M.B. Karoui, Z. Kaddachi, R. Gharbi, April Optical properties of nanostructured TiO₂ thin films, in: *Journal of Physics: Conference Series 596*, IOP Publishing, 2015, p. 12012. No. 1.
- [36] M.T. Sarode, P.N. Shelke, S.D. Gunjal, Y.B. Kholam, M.G. Takwale, S.R. Jadhkar, B.B. Kale, K.C. Mohite, P. Koinkar, Effect of annealing temperature on optical properties of titanium dioxide thin films prepared by sol-gel method, in: *International Journal of Modern Physics: Conference Series 6*, World Scientific Publishing Company, 2012, pp. 13–18.
- [37] A. Ranjitha, N. Muthukumarasamy, M. Thambidurai, R. Balasundaraprabhu, S. Agilan, Effect of annealing temperature on nanocrystalline TiO₂ thin films prepared by sol-gel dip coating method, *Optik* 124 (23) (2013) 6201–6204.
- [38] M.B. Karoui, Z. Kaddachi, R. Gharbi, Optical properties of nanostructured TiO₂ thin films, *J. Phys. Conf.* 596 (2015) (2015), 012012.
- [39] Y. Cheng, C. Lu, Y. Bai, A review on high refractive index nanocomposites for optical applications, *Recent Pat. Mater. Sci.* 4 (2011) 15 (2011).
- [40] S.R. Meher, L. Balakrishnan, Sol-gel derived nanocrystalline TiO₂ thin films: a promising candidate for self-cleaning smart window applications, *Mater. Sci. Semicond. Process.* 26 (2014) 251–258.
- [41] P. Dulian, J. Zajic, W. Żukowski, Effect of titanium source and sol-gel TiO₂ thin film formation parameters on its morphology and photocatalytic activity, *Mater. Sci. Poland* 38 (3) (2020) 424–433.
- [42] Y. Liang, S. Sun, T. Deng, H. Ding, W. Chen, Y. Chen, The preparation of TiO₂ film by the sol-gel method and evaluation of its self-cleaning property, *Materials* 11 (3) (2018) 450.
- [43] G. Womack, K. Isbilir, F. Lisco, G. Durand, A. Taylor, J.M. Walls, The performance and durability of single-layer sol-gel anti-reflection coatings applied to solar module cover glass, *Surf. Coating Technol.* 358 (2019) 76–78.
- [44] A. Afzal, A. Habib, I. Ulhasan, M. Shahid, A. Rehman, Antireflective Self-Cleaning TiO₂ Coatings for Solar Energy Harvesting Applications *Frontiers in Materials*, 2021. NA-NA.
- [45] S.P. Dalawai, M.A.S. Aly, S.S. Lathe, R. Xing, R.S. Sutar, S. Nagappan, C.S. Ha, K.K. Sadasivuni, S. Liu, Recent advances in durability of superhydrophobic self-cleaning technology: a critical review, *Prog. Org. Coating* 138 (2020) 105381.